Measurement of Geometric Phase for Mixed States Using Single Photon Interferometry

Marie Ericsson, Daryl Achilles, Julio T. Barreiro, David Branning,* Nicholas A. Peters, and Paul G. Kwiat

Department of Physics, University of Illinois at Urbana-Champaign, Urbana, Illinois 61801, USA

(Received 14 January 2004; published 7 February 2005)

Geometric phase may enable inherently fault-tolerant quantum computation. However, due to potential decoherence effects, it is important to understand how such phases arise for *mixed* input states. We report the first experiment to measure mixed-state geometric phases in optics, using a Mach-Zehnder interferometer, and polarization mixed states that are produced in two different ways: decohering pure states with birefringent elements; and producing a nonmaximally entangled state of two photons and tracing over one of them, a form of remote state preparation.

DOI: 10.1103/PhysRevLett.94.050401 PACS numbers: 03.65.Vf, 03.67.Lx, 42.65.Lm

When a pure quantum state undergoes a cyclic progression, besides the dynamical phase which depends on the evolution Hamiltonian, it retains memory of its motion in the form of a purely geometric phase factor [1,2]. This pure-state geometric phase has been experimentally demonstrated in various systems such as single-photon interferometry [3], two-photon interferometry [4], and NMR [5]. Recently, it has been proposed that fault-tolerant quantum computation may be performed using geometric phases [6], since they are independent of the speed of the quantum gate and depend only on the area of the path the state takes in Hilbert space. The next step is to investigate the resilience of geometric phases to decoherence. Some properties of geometric phases for mixed states, proposed by Sjöqvist *et al.* [7], have been recently investigated in NMR [8]. Here, we report the first experimental study of geometric phase for mixed quantum states with single photons. Because of the exquisite control achievable with optical qubits, we precisely map the behavior of the phase for various amounts of mixture, yielding experimental data in very good agreement with theoretical predictions. These results are encouraging in light of recent work on scalable linear optics quantum computation [9].

In order to measure a geometric phase, the dynamical phase has to be eliminated. One can parallel transport the state vector in order to ensure that the dynamical phase is zero at all times. The parallel transport condition for a particular state vector $|\Psi(t)\rangle$ is $\langle\Psi(t)|\dot{\Psi}(t)\rangle = 0$, which implies that there is no change in phase when $|\Psi(t)\rangle$ evolves to $|\Psi(t + dt)\rangle$, for some infinitesimal change in time t. However, even though the state does not acquire a phase locally, it can acquire a phase globally after completing a cyclic evolution. This global phase is equal to the geometric phase, and has its origin in the underlying curvature of the state space. It is therefore resilient to certain dynamical perturbations of the evolution, e.g., it is independent of the speed (or acceleration) of evolution.

Uhlmann [10] described mixed-state geometric phases in a mathematical context where the parallel transport of a mixed state is defined in a larger state space which purifies the mixed state [11]. In this approach the number of parallel transport conditions for a known $N \times N$ density matrix is N^2, but its time evolution operator has only N free variables. This approach can only be described in a larger Hilbert space with the system and an attached ancilla evolving together in a parallel manner [12].

Sjöqvist *et al.* defined a mixed-state geometric phase requiring no auxiliary subsystem [7,12]. This phase can be investigated using an interferometer in which a mixed state is parallel transported by a unitary operator in one arm; the output then interferes with the other arm, which has no geometric phase. The parallel transport of a mixed state $\rho = \sum_{k=1}^{N} p_k|k\rangle\langle k|$ is given by $\langle k(t)|\dot{k}(t)\rangle = 0, \forall k$, i.e., each eigenvector of the initial density matrix is parallel transported by the unitary operator. The resulting N conditions uniquely determine the unitary operator and ensure the gauge invariance of the geometric phase. A consequence is that each eigenvector acquires a geometric phase γ_k, and an associated interference visibility v_k. The total mixed-state geometric phase factor is the average of the individual phase factors, weighted by p_k,

$$ve^{i\gamma_g} = \sum_k p_k v_k e^{i\gamma_k}. \tag{1}$$

The polarization mixed state of a single photon can be represented by its density operator, which can be written in terms of the Bloch vector $\vec{r}$ and the Pauli matrices $\vec{\sigma} = \{\sigma_x, \sigma_y, \sigma_z\}$, as $\rho = \frac{1}{2}(\mathbf{1} + \vec{r}\cdot\vec{\sigma})$. It represents a mixture of its two eigenvectors with eigenvalues $\frac{1}{2}(1 \pm r)$. The length of the Bloch vector r gives the measure of the purity of the state, from completely mixed ($r = 0$) to pure ($r = 1$). For photons of purity r, Eq. (1) becomes

$$ve^{i\gamma_g} = \cos(\Omega/2) - ir\sin(\Omega/2), \tag{2}$$

where Ω is the solid angle enclosed by the trajectory of one of the eigenvectors on the Bloch sphere with corresponding geometric phase $\Omega/2$ (the other eigenvector traverses the same trajectory, but in the opposite direction, leading to a geometric phase $-\Omega/2$). From Eq. (2) we obtain the visibility and geometric phase, respectively, [7]

$$v = \sqrt{\cos^2(\Omega/2) + r^2\sin^2(\Omega/2)}, \text{ and} \tag{3}$$

$$\gamma_g = -\arctan(r\tan(\Omega/2)). \quad (4)$$

Note that for pure states, $\gamma_g = -\Omega/2$.

In our experiment, single-photon states are conditionally produced by detecting one member of a photon pair produced in spontaneous parametric down-conversion (SPDC) [13] (we also took data using coherent states from a diode laser). Specifically, pairs of photons at 670 nm and the conjugate wavelength 737 nm are produced via SPDC by pumping Type-I phase matched beta barium borate (BBO) with an Ar^+ laser at $\lambda = 351$ nm. By conditioning on detection of a 737-nm "trigger" photon (with an avalanche photodiode after a 5-nm FWHM interference filter at 737 nm), the quantum state of the conjugate mode is prepared into an excellent approximation of a single-photon Fock state at 670 nm [3,13], also with wavelength spread $\delta\lambda \sim 5$ nm. As shown in Fig. 1, the 670-nm photons are coupled into a single-mode optical fiber to guarantee a single spatial mode input for the subsequent interferometer. A fiber polarization controller is used to cancel any polarization transformations in the fiber.

The mixedness of the 670-nm photons is set via two different methods [14]. The first uses thick birefringent decoherers that couple the single photon's polarization to its arrival time relative to the trigger [15,16]. Consider a horizontally polarized ($|H\rangle$) and a vertically polarized ($|V\rangle$) photon. Assuming the decoherers delay vertically polarized photons relative to horizontally polarized photons by more than the photon's coherence length (given by $\lambda^2/\Delta\lambda \sim 90\ \mu$m), upon detection of the trigger photon, $|H\rangle$ will in principle be detected before $|V\rangle$. Tracing over the timing information during state detection erases coherence between these distinguishable states; this is equivalent to irreversible decoherence [14].

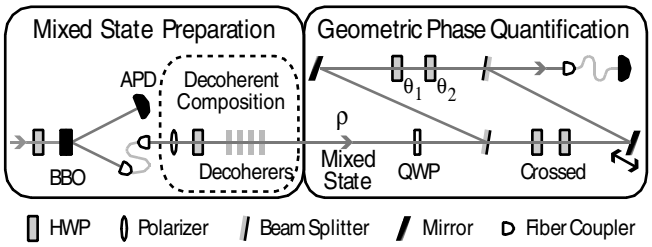

FIG. 1. Mixed-state generation and interferometer to measure geometric phase. Mixed states are prepared via two methods: (1) tracing over the polarization of one photon of a nonmaximally entangled polarization state and, (2) using an initial pure polarization state with birefringent decoherers that couple polarization to photon arrival time (see dashed box) [16]. In the latter case, tracing over this time prepares a mixed state. Half-wave plates at θ_1 and θ_2 generate geometric phase but do not otherwise alter the transmitted polarization state. Two crossed wave plates in the lower interferometer arm give no geometric phase, but compensate the optical path difference between the arms to achieve high visibility. The interferometer shape minimizes unwanted polarization changes arising from non-normal mirror and beam splitter reflections.

To guarantee a fiducial state for this method, a horizontal polarizer is placed after the polarization controller, followed by a half-wave plate (HWP), and finally the decoherers (four pieces of quartz of $\sim$3 cm total thickness). By rotating the HWP, the state can be prepared in an arbitrary superposition $\cos\theta|H\rangle + \sin\theta|V\rangle$. The light is then sent through the decoherers, effectively erasing the off-diagonal terms in the density matrix, resulting in purity $r = |\cos 2\theta|$. In our experiment, the eigenstates of the net geometric phase *operator* are circular polarizations; therefore, before entering the interferometer, the quantum state is rotated with a quarter-wave plate (QWP) into a mixture of left ($|L\rangle \equiv (|H\rangle + i|V\rangle)/\sqrt{2}$) and right ($|R\rangle \equiv (|H\rangle - i|V\rangle)/\sqrt{2}$) circular polarized light.

Our second method to produce mixed-polarization single-photon states, a version of remote state preparation [17], is to trace over one of the photons of a pair initially in a nonmaximally entangled polarization state. This state is prepared using two thin BBO crystals oriented such that pumping with polarization θ_p produces a variable entanglement superposition state $\cos\theta_p|HH\rangle + \sin\theta_p|VV\rangle$ [18]. Here, the first position polarization label corresponds to the trigger photon (at 737 nm) while the second corresponds to its partner (at 670 nm). A polarization-insensitive measurement of the trigger photon prepares the partner in the polarization mixed state $\rho_{670\,\mathrm{nm}} = \cos^2\theta_p|H\rangle\langle H| + \sin^2\theta_p|V\rangle\langle V|$, with $r = |\cos 2\theta_p|$. $\rho_{670\,\mathrm{nm}}$ is then transported over the single-mode fiber (still with the polarization controller so the fiber does not alter the state). As before, a QWP is used to rotate the photon's polarization state to a mixture of $|R\rangle$ and $|L\rangle$ before entering the interferometer.

After any of the above mixed-state preparations, the photon is sent into a Mach-Zehnder interferometer (Fig. 1). In the upper arm, the Bloch vector $\vec{r}$ is evolved unitarily using two half-wave plates with optic axes at θ_1 and θ_2, respectively. The evolution can be illustrated

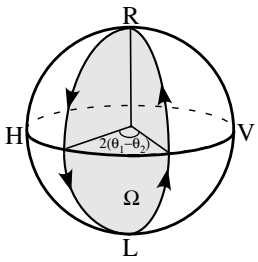

FIG. 2. The solid angle Ω enclosed by the cyclic path of one eigenvector of the density matrix. The other eigenvector traces the same path but in the opposite direction, thus enclosing the solid angle $-\Omega$. Ω can be varied by adjusting $\theta_1 - \theta_2$, the relative angle between the optic axes of the two HWPs in the geometric phase arm of the interferometer.

(Fig. 2) with one of the eigenvectors of the density matrix, e.g., $|R\rangle$, traveling along two geodesics going from $|R\rangle$ to $|L\rangle$ and back. The trajectory encloses a solid angle $\Omega = 4(\theta_1 - \theta_2)$ [19]. For mixed states, the length of r is reduced, but the same solid angle is subtended. The resulting evolution fulfills the parallel transport conditions for mixed states, and the induced geometric phase is obtained by substituting $\Omega/2 = 2\theta_1$ into Eqs. (3) and (4). A motorized rotation stage is used to set θ_1 (to within 0.01°) and thus, the geometric phase.

To measure γ_g and v, we apply a dynamical phase shift in the lower interferometer arm and measure the resulting interference pattern both with a geometric phase (for several settings of θ_1 [20]) and without ($\theta_1 = 0$). The dynamical phase shift is produced with a piezoelectric transducer (PZT) on the translation stage on which the lower path mirror is mounted. By adjusting the voltage across the PZT, the length difference (ΔL) between the arms is varied, giving the probability for the photon to exit the interferometer to the detector as

$$P(\Delta L) = (1 + v\cos(2\pi\Delta L/\lambda - \gamma_g))/2 \qquad (5)$$

Photons are detected using an avalanche photodiode. To conditionally prepare a single-photon Fock state with the desired bandwidth, we count only coincident detections (within a 4.5-ns timing window) with the trigger detector. We estimate the probability of two photons being present accidentally during a given coincidence window is 3×10^{-6} for the decoherer method (using a 4-mm thick BBO crystal) and 8×10^{-9} for the entanglement method (using two 0.6-mm crystals). Thus the ''accidental'' coincidence rate (e.g., between photons corresponding to different pairs, or from detector dark counts) is negligible, and has *not* been subtracted from the data.

Data is taken by varying the PZT voltage from 30 to 70 volts, in 5-volt steps, giving slightly more than one period of the interference pattern. At each voltage, data is accumulated for 2 s (decoherer method) or 6 s (traced-over entangled state method). We plot the number of coincidences as a function of PZT voltage, and then fit a curve to extract the phase and visibility information for each HWP setting [21]. To calculate the phase difference due to the geometric phase, we relate the data for each HWP setting θ_1 to the reference data with $\theta_1 = 0$ [see inset in Figs. 3(a) and 3(c)] [22].

The experimental data are plotted in Figs. 3(a)–3(f), along with theoretical curves based on the measured purity of the photons. To determine purity, we measure the $|H\rangle$

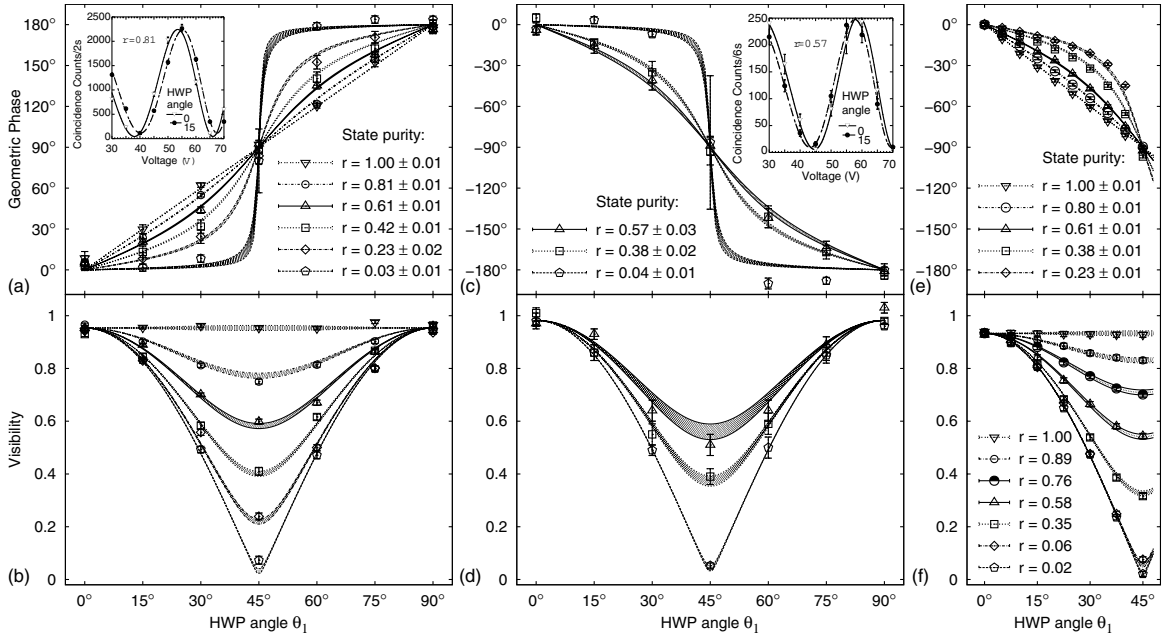

FIG. 3. The mixed-state geometric phases and visibilities as a function of the half-wave plate angle θ_1. (a),(b) The photons in the mixed-polarization state were produced with decohering quartz elements (see text). (c),(d) The mixed-polarization state photons were produced by tracing over one photon in a nonmaximally entangled state. (e),(f) The classical laser was decohered with an imbalanced polarizing interferometer. The error bars are derived from the fit of the raw data to Eq. (5). The error in the theoretical curves shown results from uncertainties in the determination of r, due to photon counting statistics [or intensity fluctuations for (e) and (f)]. The visibility theory curves are normalized to the average visibility when $\theta_1 = 0$: 95% for (b), 98% for (d), and 93% for (e). The slightly imperfect visibility is largely due to imperfect interferometer mode matching. Typical data is shown inset in (a) ($\theta_1 = 0°$ and $\theta_1 = 15°$ for $r = 0.81$) and (c) ($\theta_1 = 0°$ and $\theta_1 = 15°$, and $r = 0.57$). Note: In (a) and (c) the curves are flipped along the x axis: in the first setup the input states possessed larger right-circular polarization eigenvalues, while in the second setup, left-circular polarization was dominant [23].

and $|V\rangle$ components of the mixed state before the last quarter-wave plate in front of the interferometer. Figures 3(a) and 3(b) show the data for the geometric phase and the visibility, respectively, for the experiment where the single photons are decohered with thick birefringent quartz. Figures 3(c) and 3(d) show the corresponding data when the mixture is due to entanglement to the trigger photon. Figures 3(e) and 3(f) show results from the coherent state, indicating that the data clearly fits the theoretical prediction and demonstrates that the single-photon geometric phase survives the correspondence principle classical limit [3].

Figure 3's error bars arise from the fitting program's uncertainty estimate of the phase and visibility from the raw fringes. This error is consistent with the standard error obtained from repeating measurements 4 times to calculate the spread in the geometric phase and visibility. We quantify how well the data fits the theory using a weighted reduced χ^2 analysis. For the geometric phases (visibilities), we obtain average values of 0.98 (1.36) and 1.14 (0.94) for the decoherer and entangled state preparations, respectively, indicating an excellent fit. Also, the values of r retrodicted from our fringe data agree with our direct measurements of r within uncertainty.

We report the first measurement of geometric phases for single photons prepared in various polarization mixed states, created using two different methods. Specifically, we report a novel way of creating decohered one-qubit states from entangled two-qubit states, a simple version of remote state preparation. Both types of mixed states give geometric phase and visibility data in very good agreement with the theoretical predictions. Our results indicate that we have a good measure of the geometric phase for mixed states, which in future work will enable the estimation of fault tolerance in geometric quantum computation with linear optical elements. We also anticipate further experiments on nonunitarily evolved mixed states [12] and non-Abelian geometric phases [24], to ultimately realize a universal set of geometric gates for quantum computation [25].

We thank J. B. Altepeter, E. R. Jeffrey, A. VanDevender, and T.-C. Wei for valuable discussions and technical assistance. M. E. acknowledges financial support from The Foundation BLANCEFLORBoncompagni-Ludovisi, née Bildt. We recognize partial support from the National Science Foundation (Grant No. EIA-0121568).

*Present address: Department of Physics and Optical Engineering, Rose-Hulman Institute of Technology, Terre Haute, IN, 47803, USA

[1] S. Pancharatnam, Proc. Indian Acad. Sci. A **44**, 247 (1956).
[2] M. V. Berry, Proc. R. Soc. London A **392**, 45 (1984).
[3] P. G. Kwiat and R. Y. Chiao, Phys. Rev. Lett. **66**, 588 (1991).
[4] J. Brendel, W. Dultz, and W. Martienssen, Phys. Rev. A **52**, 2551 (1995); D. V. Strekalov and Y. H. Shih, Phys. Rev. A **56**, 3129 (1997).
[5] D. Suter, K. T. Mueller, and A. Pines, Phys. Rev. Lett. **60**, 1218 (1988).
[6] J. A. Jones *et al.*, Nature (London) **403**, 869 (2000); P. Zanardi and M. Rasetti, Phys. Lett. A **264**, 94 (1999); L. M. Duan, J. I. Cirac, and P. Zoller, Science **292**, 1695 (2001); S.-L. Zhu and Z. D. Wang, Phys. Rev. Lett. **91**, 187902 (2003).
[7] E. Sjöqvist *et al.*, Phys. Rev. Lett. **85**, 2845 (2000).
[8] J. Du *et al.*, Phys. Rev. Lett. **91**, 100403 (2003).
[9] E. Knill, R. Laflamme, and G. Milburn, Nature (London) **409**, 46 (2001); T. B. Pittman, B. C. Jacobs, and J. D. Franson, Phys. Rev. Lett. **88**, 257902 (2002); T. B. Pittman *et al.*, Phys. Rev. A **68**, 032316 (2003); J. L. O'Brien *et al.*, Nature (London) **426**, 264 (2003).
[10] A. Uhlmann, Rep. Math. Phys. **24**, 229 (1986).
[11] M. A. Nielsen and I. L. Chuang, *Quantum Computation and Quantum Information* (Cambridge University Press, Cambridge, England, 2000), p. 109.
[12] M. Ericsson *et al.*, Phys. Rev. Lett. **91**, 090405 (2003).
[13] C. K. Hong and L. Mandel, Phys. Rev. Lett. **56**, 58 (1986).
[14] P. G. Kwiat and B.-G. Englert, in *Science and Ultimate Reality*, edited by J. D. Barrow, P. C. W. Davies, and C. L. Harper, Jr. (Cambridge University Press, Cambridge, England, 2004).
[15] A. J. Berglund, B.A. thesis, Dartmouth College, 2000, also quant-ph/0010001; N. Peters *et al.*, Quantum Inf. Comput. **3**, 503 (2003).
[16] The classical light is similarly mixed, using an unbalanced polarizing interferometer to separate $|H\rangle$ and $|V\rangle$ by more than the ~ 1 *m* diode laser coherence length.
[17] C. H. Bennett *et al.*, Phys. Rev. Lett. **87**, 077902 (2001).
[18] P. G. Kwiat *et al.*, Phys. Rev. A **60**, R773 (1999).
[19] We can fix $\theta_2 = 0$, since Ω depends only on $\theta_1 - \theta_2$.
[20] The adjustable wave plate must not be wedged, or the path overlap will be ruined when the wave plate is rotated.
[21] Because the voltage applied to the PZT creates a nonlinear increase in the path length, we fit our data to a sinusoid with nonlinear dependence on the argument. The PZT nonlinear fit parameters were determined by measuring dynamical phase fringes in our interferometer.
[22] To reduce the effect of dynamical phase drift, the reference data is taken both before and after each geometric phase-generating HWP setting. The data for each specific wave plate setting is used to calculate the geometric phase relative to both the initial and final reference data; the reported result is the average of the two calculations.
[23] The $r = 0.04$ initial state was prepared more right-circular polarized than left, opposite of the initial states for the $r = 0.38$ and $r = 0.57$ trials. Therefore, for ease of comparison with these curves, the $r = 0.04$ data curve is displayed flipped about the horizontal.
[24] F. Wilczek and A. Zee, Phys. Rev. Lett. **52**, 2111 (1984).
[25] J. Pachos, P. Zanardi, and M. Rasetti, Phys. Rev. A **61**, 010305(R) (1999).